ACS chemical biology

pubs.acs.org/acschemicalbiology

Articles

S-Adenosylmethionine (SAM)-Dependent Methyltransferase MftM is Responsible for Methylation of the Redox Cofactor Mycofactocin

Mark Ellerhorst, Stefanie A. Barth, Ana Patrícia Graça, Walid K. Al-Jammal, Luis Peña-Ortiz, Ivan Vilotijevic, and Gerald Lackner*

Cite This: *ACS Chem. Biol.* 2022, 17, 3207−3217

Read Online

ACCESS | Metrics & More | Article Recommendations | Supporting Information

ABSTRACT: Mycobacteria produce several unusual cofactors that contribute to their metabolic versatility and capability to survive in different environments. Mycofactocin (MFT) is a redox cofactor involved in ethanol metabolism. The redox-active core moiety of mycofactocin is derived from the short precursor peptide MftA, which is modified by several maturases. Recently, it has been shown that the core moiety is decorated by a β-1,4-glucan chain. Remarkably, the second glucose moiety of the oligosaccharide chain was found to be 2-*O*-methylated in *Mycolicibacterium smegmatis*. The biosynthetic gene responsible for this methylation, however, remained elusive, and no methyltransferase gene was part of the MFT biosynthetic gene cluster. Here, we applied reverse genetics to identify the gene product of MSMEG_6237 (*mftM*) as the SAM-dependent methyltransferase was responsible for methylation of the cofactor in *M. smegmatis*. According to metabolic analysis and comparative genomics, the occurrence of methylated MFT species was correlated with the presence of *mftM* homologues in the genomes of mycofactocin producers. This study revealed that the pathogen *Mycobacterium tuberculosis* does not methylate mycofactocins. Interestingly, *mftM* homologues co-occur with both mycofactocin biosynthesis genes as well as the putative mycofactocin-dependent alcohol dehydrogenase Mdo. We further showed that *mftM* knock-out mutants of *M. smegmatis* suffer from a prolonged lag phase when grown on ethanol as a carbon source. In addition, in vitro digestion of the glucose chain by cellulase suggested a protective function of glucan methylation. These results close an important knowledge gap and provide a basis for future studies into the physiological functions of this unusual cofactor modification.

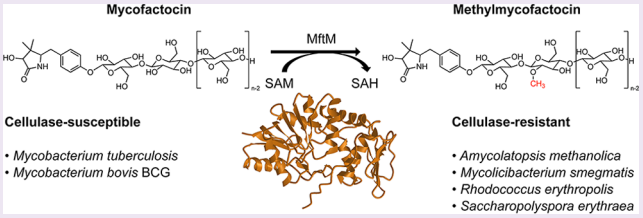

INTRODUCTION

Mycofactocin (MFT) is a redox cofactor involved in ethanol metabolism in mycobacteria. When biosynthetic genes of the cofactor are inactivated, both *M. smegmatis* and *M. tuberculosis* fail to utilize ethanol as a carbon source.[1] Involvement of MFT in methylotrophy was also reported for a strain of *M. smegmatis*.[2] Given the low amount of endogenous ethanol in animal tissues,[3] obligate pathogens like *M. tuberculosis* encounter considerable amounts of alcohol only after intake of exogenous ethanol, which readily reaches the airways, a hotspot of TB infection.[4] A recent study showed significant effects of the MFT locus on the growth and pathogenicity of *M. tuberculosis* in the absence of exogenous ethanol, thus pointing toward further roles of MFT in mycobacteria.[5] Notably, induction of MFT biosynthesis genes by long-chain fatty acyl-CoA esters suggests an involvement in fatty acid metabolism.[6]

The biosynthetic pathway to MFT comprises at least six gene products (MftA-F) (Figure 1A) and follows the logic of ribosomally synthesized and post-translationally modified peptide (RiPP) biosynthesis.[7,8] After translation by the ribosome, the precursor peptide MftA (MSMEG_RS06945) is bound by its chaperone MftB (MSMEG_1422) and modified at its C-terminus by the radical *S*-adenosylmethionine (rSAM) enzyme MftC (MSMEG_1423, Figure 1B).[9,10] This reaction was studied in detail in vitro and was shown to be a combination of oxidative decarboxylation and cyclization of the C-terminal valine−tyrosine core peptide.[11] The modified core is then cleaved by the peptidase MftE (MSMEG_1425),[12,13] leading to the cyclic intermediate 3-amino-5[(*p*-hydroxyphenyl)methyl]-4,4-dimethyl-2-pyrrolidinone (AHDP),[13] which is finally oxidatively deaminated to form the cyclic keto amide premycofactocin (PMFT).[14] The latter is redox-active, and it is reduced by a carveol dehydrogenase to its reduced form $PMFTH_2$. Investigations of living cultures of *M. smegmatis* by ^{13}C-labeling and LC-MS-based metabolomics revealed MFT derivatives carrying a β-1,4-glucan chain consisting of up to nine glucose units.[15] These glycosylated MFT congeners were termed MFT-*n*, with n

Received: August 22, 2022
Accepted: October 6, 2022
Published: October 26, 2022

ACS Publications

© 2022 The Authors. Published by American Chemical Society

https://doi.org/10.1021/acschembio.2c00659
ACS Chem. Biol. 2022, 17, 3207−3217

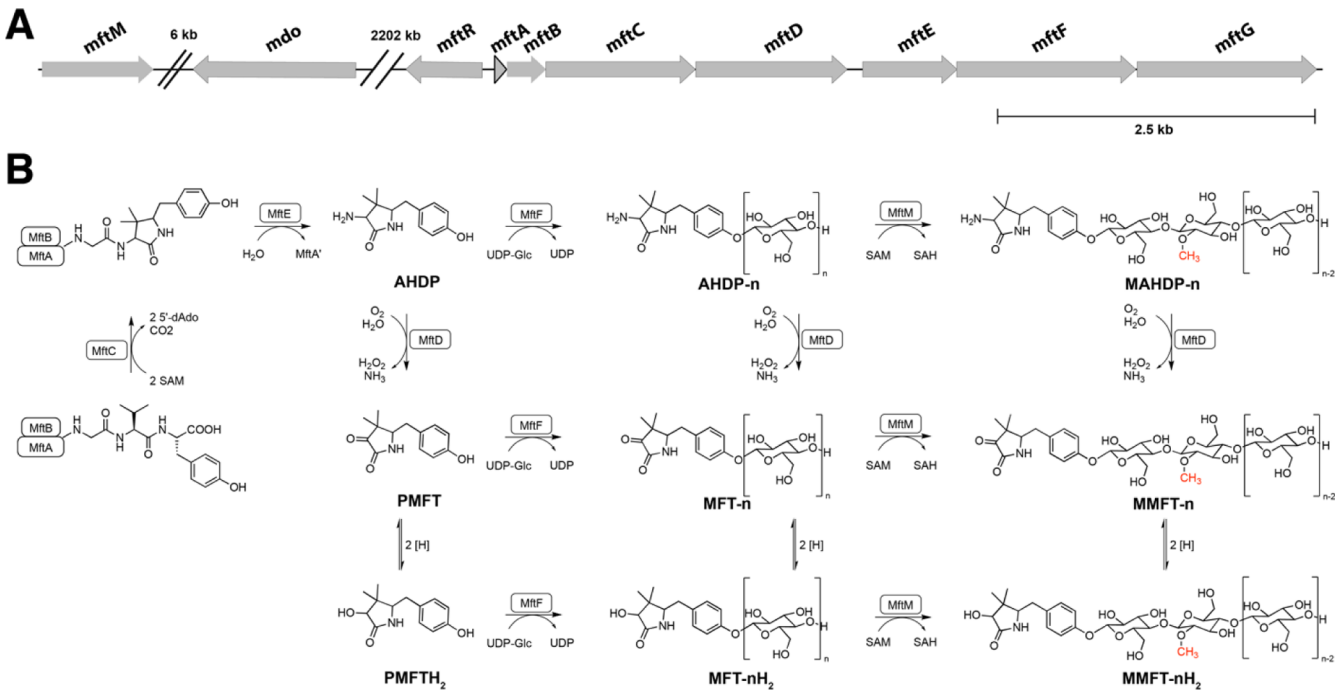

Figure 1. Biosynthesis of mycofactocin in *M. smegmatis*. (A) BGC of MFT in *M. smegmatis* mc^2 155 comprising the genes *mftABCDEF*, the glucose-methanol-choline family oxidoreductase gene *mftG*, and the transcriptional regulator gene *mftR*. The genes *mftM* (methyltransferase) and *mdo* (mycofactocin-dependent alcohol dehydrogenase) are located in a distinct gene cluster. (B) Proposed MFT biosynthesis model. AHDP: 3-amino-5[(*p*-hydroxyphenyl)methyl]-4,4-dimethyl-2-pyrrolidinone, PMFT: premycofactocinone, PMFTH$_2$: premycofactocinol, MFT-*n*: mycofactocinone, MFT-*n*H$_2$: mycofactocinol, MMFT-*n*: methylmycofactocinone, MMFT-*n*H$_2$: methylmycofactocinol, UDP-Glc: uridine diphosphate glucose, SAH: *S*-adenosylhomocysteine, SAM: *S*-adenosylmethionine, MftA: mycofactocin precursor peptide, MftA′: cleavage product of MftA after MftC reaction, MftB: peptide chaperone, MftC: radical SAM decarboxylase/cyclase, MftD: AHDP deaminase, MftE: peptidase, MftF: glycosyltransferase, and MftM: SAM-dependent methyltransferase discovered in this study.

indicating the number of glucose moieties. As expected for a redox cofactor, they occurred in both oxidized (mycofactocinones, MFT-*n*) and reduced forms (mycofactocinols, MFT-*n*H$_2$) and—similar to the aglycones—were successfully reduced by carveol dehydrogenase.[15] These findings supported the hypothesis that mycofactocins are redox cofactors as initially proposed by bioinformatics.[8] The attachment of the β-1,4-glucan, mediated by the glycosyltransferase MftF (MSMEG_1426),[15] may enhance interactions with enzymes or avoid leakage from cells. Curiously, the β-1,4-glucan of mycofactocins and its biosynthetic precursor AHDP-n exhibited further modification. The 2-hydroxyl group of the second glucose moiety was methylated in the majority of mycofactocin species, resulting in methylmycofactocins (MMFT-*n*, MMFT-*n*H$_2$).[6,15] This finding was surprising since no methyltransferase was encoded in the MFT biosynthetic gene cluster (BGC) of *M. smegmatis*. Here, we report the discovery of the *mftM* gene (MSMEG_6237) encoding the methyltransferase responsible for MFT methylation in *M. smegmatis* and showing that the presence or absence of *mftM* homologues correlates with MMFT production in various microorganisms, revealing the absence of methylmycofactocins in the human pathogen *M. tuberculosis*.

RESULTS AND DISCUSSION

Candidate Selection for Identification of Mycofactocin Methyltransferase. As outlined above, the enzyme responsible for methylation of mycofactocin remained elusive. As a first experiment, the metabolic origin of the methyl group was attempted to be identified. This was performed by stable isotope labeling in vivo by feeding *M. smegmatis* with L-methionine-(methyl-^{13}C), which is a direct precursor of *S*-adenosylmethionine in vivo. To increase the specificity of isotopic labeling, two core amino acids of MftA, L-tyrosine, and L-valine were fed as fully ^{13}C-labeled precursors (L-valine-$^{13}C_5$ and L-tyrosine-$^{13}C_9$), leading to the incorporation of 13 ^{13}C atoms into mycofactocins as shown before.[15] The analysis of cell extracts by liquid chromatography−mass spectrometry (LC−MS) revealed a mass shift for methylmycofactocins of +14.0498 *m*/*z* (Figure 2A,B and Figure S1), suggesting one additional ^{13}C label derived from L-methionine-(methyl-^{13}C) in the glycosyl chain. This result was compatible with the assumption that the *O*-methylation is catalyzed by *S*-adenosyl methionine (SAM)-dependent methyltransferase.[16]

The identification of the gene, however, was hampered by the fact that over 100 putative methyltransferases were annotated in the genome of *M. smegmatis*. From these genes, seven candidates (Table 1) matching one of the following criteria were selected for gene inactivation: (1) transcriptional upregulation in the presence of ethanol, which is known to induce the biosynthesis of mycofactocin,[1,15] (2) proximity to oligosaccharide-modifying gene clusters, or (3) proximity to genes associated with mycofactocin.

Mycofactocin Methyltransferase Candidate Knock-Out Analysis. The selected seven candidate genes were all subjected to targeted gene deletion by double-cross-over and subsequent metabolome analysis by LC−MS to assess the capability of resulting mutants to form methylmycofactocins. Strikingly, the mutant *M. smegmatis* ΔMSMEG_6237 showed the complete absence of methylmycofactocins in

https://doi.org/10.1021/acschembio.2c00659
ACS Chem. Biol. 2022, 17, 3207−3217

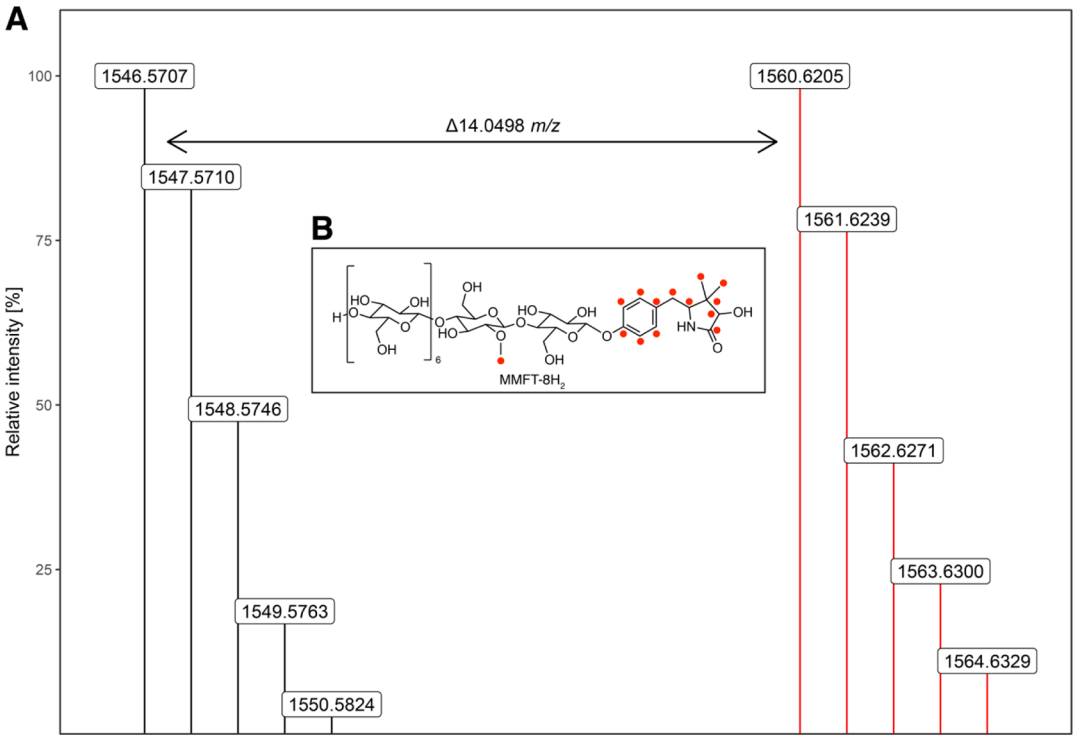

Figure 2. Stable isotope labeling followed by LC−MS demonstrating methyl transfer from L-methionine-(methyl-^{13}C) to methylmycofactocin. (A) Shown are isotope distribution patterns of MMFT-8H_2 ($C_{62}H_{99}NO_{43}$, m/z 1546.5664 [M + H]$^+$, 2.8 ppm) of the unlabeled monoisotopic molecule and of the fully labeled molecule (m/z 1560.6134 [M + H]$^+$, 0.1 ppm) from *M. smegmatis* wild-type cells fed with L-valine-$^{13}C_5$, L-tyrosine-$^{13}C_9$, and L-methionine-(methyl-^{13}C). The mass shift of m/z 14.0498 corresponds to the incorporation of 14 ^{13}C atoms (13 from the MFT aglycone core and 1 in the glycosyl chain). In black, the isotope pattern of the unlabeled control, and in red, the isotope pattern of the stable isotope-labeled metabolome extracts, are shown (originating from two independent experiments). (B) Structure of MMFT-8H_2 with ^{13}C-labeled atoms highlighted in red. Parts per million (ppm) values indicate relative mass deviations.

Table 1. Methyltransferase Encoding Genes Investigated in This Study[a]

candidate	locus tag	protein accession number UniProt identifier	length (aa)	protein family/UniProt annotation	criterion
1	MSMEG_1650	WP_011727800.1 A0QSY9	245	PF08241/methyltransferase type 11	1
2	MSMEG_1771	WP_011727889.1 A0QTA5	222	No PFAM domain annotated/methylase, putative	1
3	MSMEG_5176	WP_011730362.1 A0R2N4	216	PF08241/methyltransferase type 11	1
4	MSMEG_5354	WP_003896752.1 A0R360	341	PF00891/*O*-methyltransferase, family protein 2	2
5	MSMEG_6235	WP_029104596.1 A0R5L6	226	PF13649/thiopurine *S*-methyltransferase (Tpmt) superfamily protein	3
6	**MSMEG_6237**	**WP_011731146.1** A0R5L7	**293**	**PF08241/methyltransf_11 domain-containing protein**	**3**
7	MSMEG_6663	WP_011731441.1 A0R6T3	247	PF08241/C5-*O*-methyltransferase	1

[a]The MFT methyltransferase MftM is shown in bold. UniProt annotations are the most recent and do not represent the status during candidate selection. Protein family annotations: PF08241: methyltransf_11—SAM-dependent methyltransferase domain, PF00891: methyltransf_2—*O*-methyltransferase domain, PF13649: methyltransf_25—methyltransferase domain. Protein family annotations were obtained from InterPro version 89.0. aa: amino acids. Criteria: (1) transcriptional upregulation in the presence of ethanol,[1] (2) proximity to oligosaccharide-modifying genes, or (3) proximity to genes associated with mycofactocin.

ΔMSMEG_6237, while non-methylated MFTs were still produced. The inactivation of the other six candidate genes did not show any interference with MFT biosynthesis (Figure 3 and Figure S2). This result provided evidence that MSMEG_6237 (WP_011731146.1) is indeed responsible for the methylation of mycofactocin. We therefore propose *mftM* as an appropriate name for MSMEG_6237 and its functional homologues. The complementation of the knock-out strain by re-introduction of the *mftM* gene via an integrative vector (Δ*mftM attB*::pMCpAINT-*mftM*, short: Δ*mftM*-comp) led to complete restoration of methylmycofactocin formation (Figure 3). Notably, *mftM* is encoded 6 kb upstream of the (postulated) mycofactocin-associated alcohol dehydrogenase gene MSMEG_6242, which was shown to be essential for the growth of *M. smegmatis* on ethanol as the sole carbon source.[1] The deduced MftM protein contains a methyltransferase 11 domain (PFAM08241) as well as a SAM binding site according to the InterPro database (version 89.0), providing further evidence that the methyl group donor for the methylation of MFT is indeed SAM. A homology search for the closest experimentally characterized homologue of MftM revealed RebM,[17] the demethylrebeccamycin-D-glucose *O*-methyltransferase from *Lentzea aerocolonigenes* (36.19% identical, Figure S3), supporting the hypothesis that their common ancestor might already have been involved in oligosaccharide modifications. To investigate if the transcription of

https://doi.org/10.1021/acschembio.2c00659
ACS Chem. Biol. 2022, 17, 3207−3217

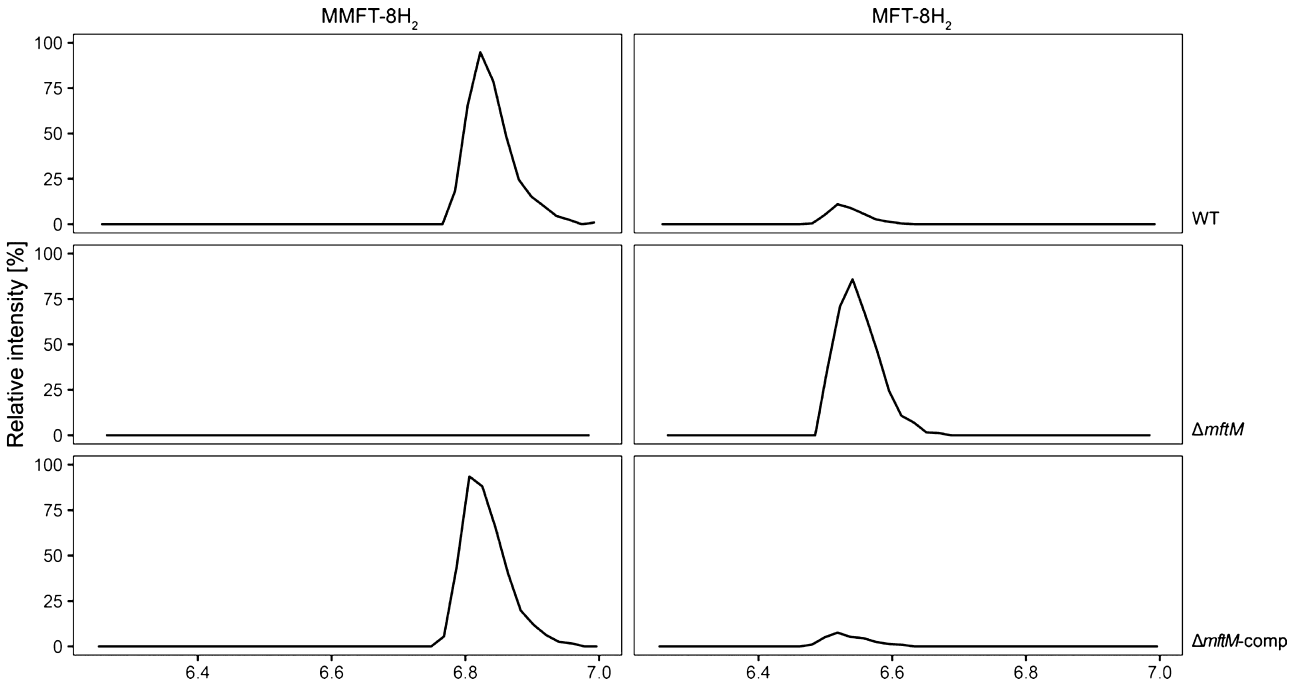

Figure 3. Gene deletion of *mftM* in *M. smegmatis* abolishing methylmycofactocin formation. Stacked extracted ion chromatograms (EICs, 5 ppm window) for methylmycofactocinol-8 (MMFT-8H_2, sum formula: $C_{62}H_{99}NO_{43}$, RT: 6.81 min, m/z 1546.5664 $[M + H]^+$) and for mycofactocinol-8 (MFT-8H_2, sum formula: $C_{61}H_{97}NO_{43}$, retention time (RT): 6.50 min, m/z 1532.5507 $[M + H]^+$) obtained from metabolome extracts of the genotypes indicated on the right. The results show the absence of methylated mycofactocins in *M. smegmatis* Δ*mftM* in contrast to the wild-type and complementation mutant Δ*mftM*-comp. Relative intensities were normalized to the maximal intensity. The figure shows one representative chromatogram out of four independent experiments. Chromatograms of all replicates are shown in Figure S2.

Table 2. Mycofactocin Congeners Found in Different Organisms Encoding an MFT Biosynthetic Gene Cluster[a]

organism	MftM homologue (protein)	methylation	mycofactocin congeners (selected adducts detected by LC−MS)					
			congener	adduct	RT [min]	calculated m/z	measured m/z	mass deviation [ppm]
A. methanolica 239	WP_017984504.1	yes	MMFT-8H_2	$[M + 2H]^{2+}$	6.76	773.7868	773.7884	2.1
M. smegmatis mc² 155	WP_011731146.1	yes	MFT-8H_2	$[M + H]^+$	6.52	1532.5507	1532.5522	1.0
			MMFT-2H_2	$[M + H]^+$	7.13	574.2494	574.2505	1.9
			MMFT-7	$[M + H]^+$	7.21	1382.4979	1382.5002	1.7
			MMFT-7H_2	$[M + H]^+$	6.86	1384.5135	1384.5156	1.5
			MMFT-8	$[M + H]^+$	7.16	1544.5507	1544.5527	1.3
			MMFT-8H_2	$[M + H]^+$	6.81	1546.5664	1546.5658	0.4
Mycobacterium bovis BCG	not detected	no	MFT-7H_2	$[M + H]^+$	6.56	1370.4979	1370.5052	5.3
M. tuberculosis H37Rv	not detected	no	MFT-7H_2	$[M + H]^+$	6.54	1370.4979	1370.5059	5.8
R. erythropolis DSM 43060	WP_019744254.1	yes	MMFT-7H_2	$[M + 2H]^{2+}$	6.86	692.7604	692.7617	1.9
			MMFT-8	$[M + H]^+$	7.18	1544.5507	1544.5553	3.0
			MMFT-8H_2	$[M + 2H]^{2+}$	6.81	773.7868	773.7885	2.2
			MMFT-9H_2	$[M + 2H]^{2+}$	6.77	854.8132	854.8155	2.7
S. erythraea NRRL2338	WP_009947194.1	yes	MMFT-2	$[M + H]^+$	7.54	572.2338	572.2371	5.8
			MMFT-2H_2	$[M + H]^+$	7.14	574.2494	574.2514	3.5
			MMFT-3	$[M + H]^+$	7.45	734.2866	734.2906	5.5

[a]Only features confirmed by both RT and MS^2 fragmentation spectra are shown.

MSMEG_6237 could be regulated by the recently characterized mycofactocin-system transcriptional regulator MftR,[6] the upstream region of MSMEG_6237 was searched for the proposed binding motif of MftR. However, no potential recognition site was found, indicating that the transcription of *mftM* in *M. smegmatis* might be regulated independently of mycofactocin biosynthesis.

Occurrence of *mftM* Homologues and Methylmycofactocins in MFT-Producing Organisms. To further investigate if the presence of *mftM* homologues is correlated with the presence of methylmycofactocins in other putative MFT-producing organisms, the occurrence of the *mftM* homologues among all organisms encoding a MFT BGC was investigated by sequence similarity (BLAST) searches in sequenced bacterial genomes. Indeed, a variety of actino-

https://doi.org/10.1021/acschembio.2c00659
ACS Chem. Biol. 2022, 17, 3207−3217

bacteria encoded homologues of the *mftM* gene of *M. smegmatis,* with a pairwise identity of the corresponding protein of >35%. So far, the in vivo biosynthesis of mycofactocins was shown only for *M. smegmatis*.[15] To experimentally examine the methylation status of mycofactocins in a selection of further organisms carrying *mftM* genes, we chose five more organisms encoding a MFT BGC: *Amycolatopsis methanolica*, *Mycobacterium bovis BCG*, *M. tuberculosis*, *Rhodococcus erythropolis*, and *Saccharopolyspora erythraea*, thus covering a wide range of actinobacterial clades. To induce MFT production, we cultivated these bacteria in the presence of ethanol. Extracted metabolomes of the cultures were investigated for the presence of MFTs by targeted LC–MS/MS and by comparison to known mycofactocin fragmentation spectra. Following this approach, we could identify MFTs as known from *M. smegmatis* in all investigated organisms, such as mycofactocinol-7 (Table 2 and Figures S4–S10). Furthermore, this analysis showed that the presence of methylmycofactocins such as methylmycofactocin-8 indeed correlated with the presence of *mftM* homologues. For example, *R. erythropolis* containing an *mftM* homologue produced methylmycofactocins, while *M. tuberculosis* lacking *mftM* homologues did not produce any detectable amounts of methylmycofactocins.

Notably, the *mftM* genes present in *R. erythropolis* and *S. erythraea* were located in the proximity of the MFT biosynthesis locus. In *M. smegmatis* and in *A. methanolica*, however, *mftM* was clustered with the *mdo* gene, that is, the gene encoding a putative mycofactocin-dependent alcohol dehydrogenase (MSEMG_6242).[1] Intriguingly, all methylating strains investigated here (*M. smegmatis*, *A. methanolica*, *R. erythropolis*, and *S. erythraea*) possess *mdo* homologues, while *M. tuberculosis* and *M. bovis* lack both *mdo* and *mftM*. To investigate correlations between *mdo*, *mftM,* and *mftC* (as a proxy for MFT biosynthesis) in a broader dataset, we analyzed their co-occurrence in complete microbial genomes containing homologues of at least one of the three genes according to BLAST searches (Figure 4 and Table S1). Strikingly, all of the complete bacterial genomes harboring *mftM* or *mdo* also

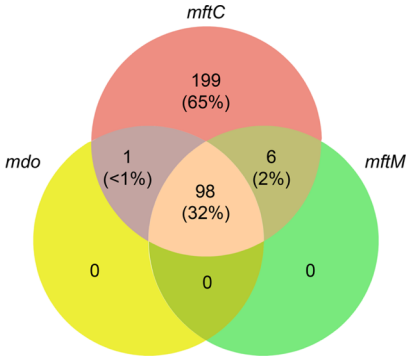

Figure 4. Co-occurrence of *mftC*, *mftM,* or *mdo* homologues in complete bacterial genomes. The Venn diagram shows the occurrence of *mftC*, *mftM,* or *mdo* in 304 genomes containing at least one of the three genes based on the similarity of their deduced proteins (n = 304). Only genomes containing *mftC* harbor *mftM* and *mdo* homologues, reflecting the functional relationship of their corresponding proteins with mycofactocin. Furthermore, *mftM* and *mdo* genes strongly tend to co-occur ($p < 0.001$). Percentages indicated in intersections describe the fraction of genomes in which the respective genes co-occur.

contained *mftC*, thus mirroring their postulated functional link to the latter. Our analysis also showed that only around one third of genomes harboring *mftC* contain an *mftM* (or *mdo*) homologue as well. In the genus *Mycolicibacterium*, 29% of (putative) MFT-producing strains contained *mftM* or *mdo*. An especially high proportion of mycofactocin producers harboring *mftM* and *mdo* was found in the genus *Rhodococcus* (90%), while in the genus *Mycobacterium*, only 9% of the species contained these genes (Table S1). This result confirms the notion that methylation of MFT is an optional but not uncommon modification performed by some organisms. The genomic association of *mdo* and *mftM* was further confirmed by our co-occurrence analysis. In 99% of the genomes harboring *mdo*, *mftM* is present as well. Of all potential MFT producers, the majority harbor either both genes together or none of them. This particular link is not restricted to a narrow phylogenetic clade within the actinobacteria but is found in diverse genera like *Mycolicibacterium*, *Streptomyces*, or *Nocardioides*. Thus, it appears unlikely that the two genes were linked just recently. Rather, their association has existed over a longer evolutionary time period and is based on either coupled gene loss or joint horizontal transfer. Future studies will have to show if the correlations between Mdo-dependent alcohol metabolism and MFT methylation are based on a direct functional link.

Physiological Effects of Mycofactocin Methylation. After the successful identification of the MFT methyltransferase, we had mutants on hand to investigate the impact of the 2-*O*-methylation on alcohol utilization in the model organism *M. smegmatis*. To this end, we monitored the growth of *M. smegmatis* wild type and Δ*mftM* on ethanol as the sole carbon source. Intriguingly, we observed a significantly longer lag phase for the knock-out strain (an increase of circa 28 h compared to the wild type) after transfer from glucose-containing to ethanol-containing media. The growth delay was completely eliminated by genetic complementation (Figure 5A) and was not observed for any other methyltransferase knock-out mutant generated in this study (Figure S11). To understand if the growth delay was correlated with an altered MFT biosynthesis, we investigated mycofactocin levels over the course of cultivation in the wild-type strain and Δ*mftM* (Figure 5B,C). This experiment revealed not only growth but also biosynthesis of mycofactocins to be delayed during the lag phase of the knock-out strain. In contrast to the mutant, wild-type and complement strains produced methylmycofactocinones and methylmycofactocinols already during the early growth phase (before 36 h). It is thus plausible that methylation of MFTs has a stimulatory effect on MFT biosynthesis via regulatory mechanisms. In this scenario, the delayed MFT biosynthesis would cause the growth phenotype. In the light of the genomic co-occurrence of *mftM* and *mdo,* it is possible that Mdo from *M. smegmatis* is directly or indirectly involved in this process.

Impact of Methylation on Mycofactocin Glycoside Stability. We have shown before that the glycosyl-chain of mycofactocin is a β-1,4-linked oligosaccharide, which serves as a target for cellulases.[15] Thus, it appeared plausible that methylation of one glucose unit could confer resistance to glycoside hydrolases that degrade the β-1,4-glucan (Figure 6A). To test this hypothesis, an extract containing methylated and non-methylated MFTs was treated with a commercially available cellulase as described previously.[15] After treatment, the long-chain mycofactocin species, including methylated and

https://doi.org/10.1021/acschembio.2c00659
ACS Chem. Biol. 2022, 17, 3207−3217

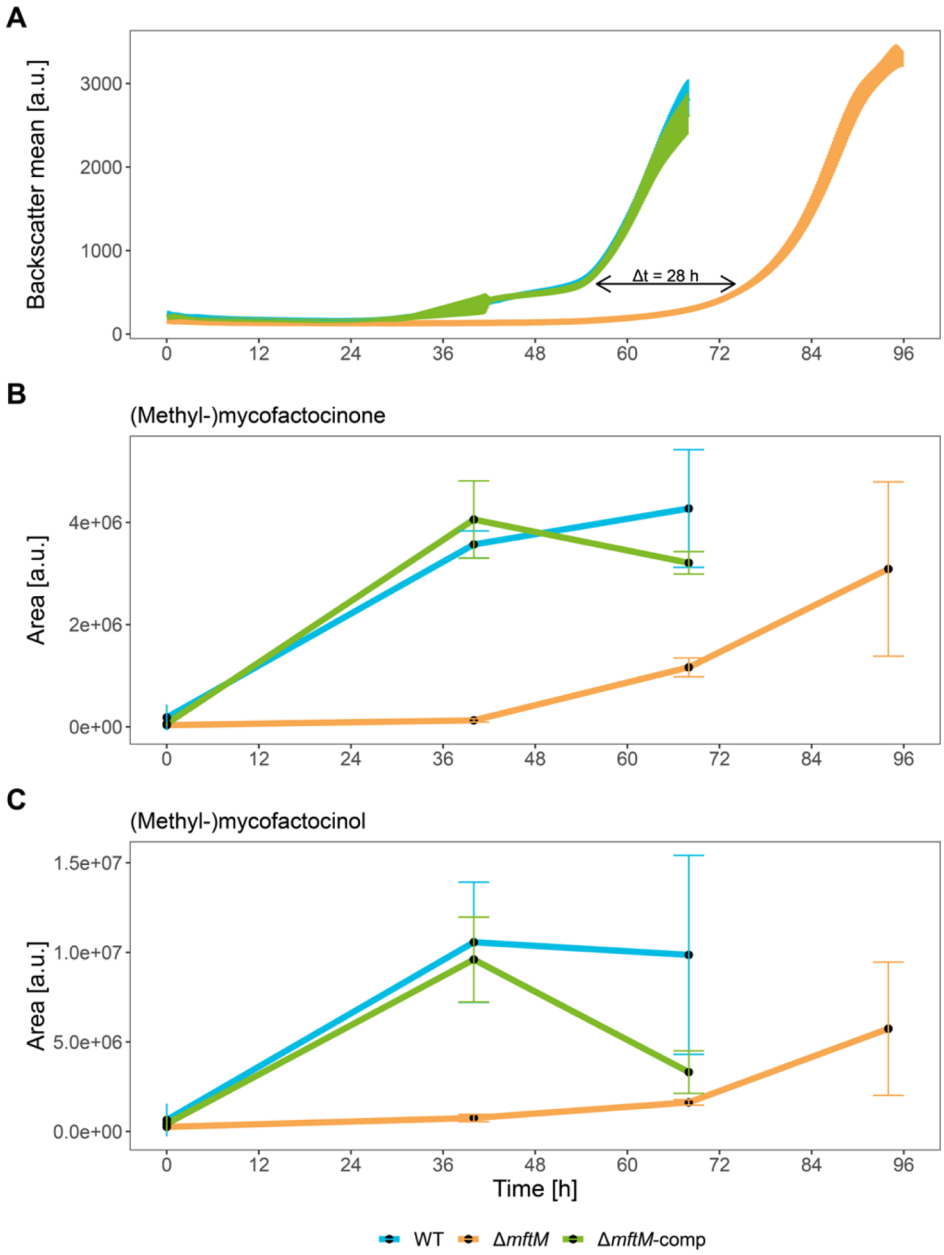

Figure 5. Growth and mycofactocin levels in *M. smegmatis* WT and *mftM* mutants. (A) Growth of *M. smegmatis* wild type, Δ*mftM* mutant, and the Δ*mftM*-comp complement strain in liquid culture on ethanol as the sole carbon source. The growth of Δ*mftM* is delayed by 28 h. Data represent quadruplicates with standard deviation as error bars. (B,C) The Δ*mftM* mutant strain displays delayed mycofactocin biosynthesis. Each time point represents the average of quadruplicates of the sum of integrated peak areas of all (B) reduced or (C) oxidized mycofactocin congeners as $[M + H]^+$ adducts in metabolome extracts normalized to cell density. For WT and complement, the sum of methylated and non-methylated forms is shown. In the Δ*mftM* mutant, only non-methylated MFTs are present.

non-methylated species, disappeared, while the aglycones PMFT and $PMFTH_2$ and the methylated methylmycofactocin-2 (MMFT-$2H_2$) accumulated (Figure 6B). It should be mentioned that during the analysis, we observed mass traces that matched the expected mass of the aglycones but eluted at different retention times in untreated samples. Chemical synthesis of the aglycones PMFT and $PFMTH_2$ finally proved that the peaks eluting at 7.8 and 8.4 min, respectively, corresponded to the aglycones. The other isobaric signals co-eluted with long-chain (M)MFTs and could thus be explained as in-source fragments of the latter. In-source fragmentation could also explain an isobaric peak of MMFT-$2H_2$, which disappeared after cellulase treatment. To investigate whether this degradation pattern is unique to mycofactocins from *M. smegmatis*, the cellulase treatment was conducted with extracts from all other strains listed in Table 2. As expected, cellulase treatments of samples from all those strains encoding an *mftM* homologue showed the same results as described for *M. smegmatis*. Samples from *M. tuberculosis* and *M. bovis*, however, which do not methylate, were completely degraded to the aglycone (Figures S12−S16). We therefore assume that the aglycones originate from non-methylated mycofactocins while methylmycofactocin-2 is a degradation product of methylated mycofactocins, such as methylmycofactocin-8, the main mycofactocin species in *M. smegmatis*. In other words, cellulase degradation of the β-1,4-glucan chain is either complete or

https://doi.org/10.1021/acschembio.2c00659
ACS Chem. Biol. 2022, 17, 3207−3217

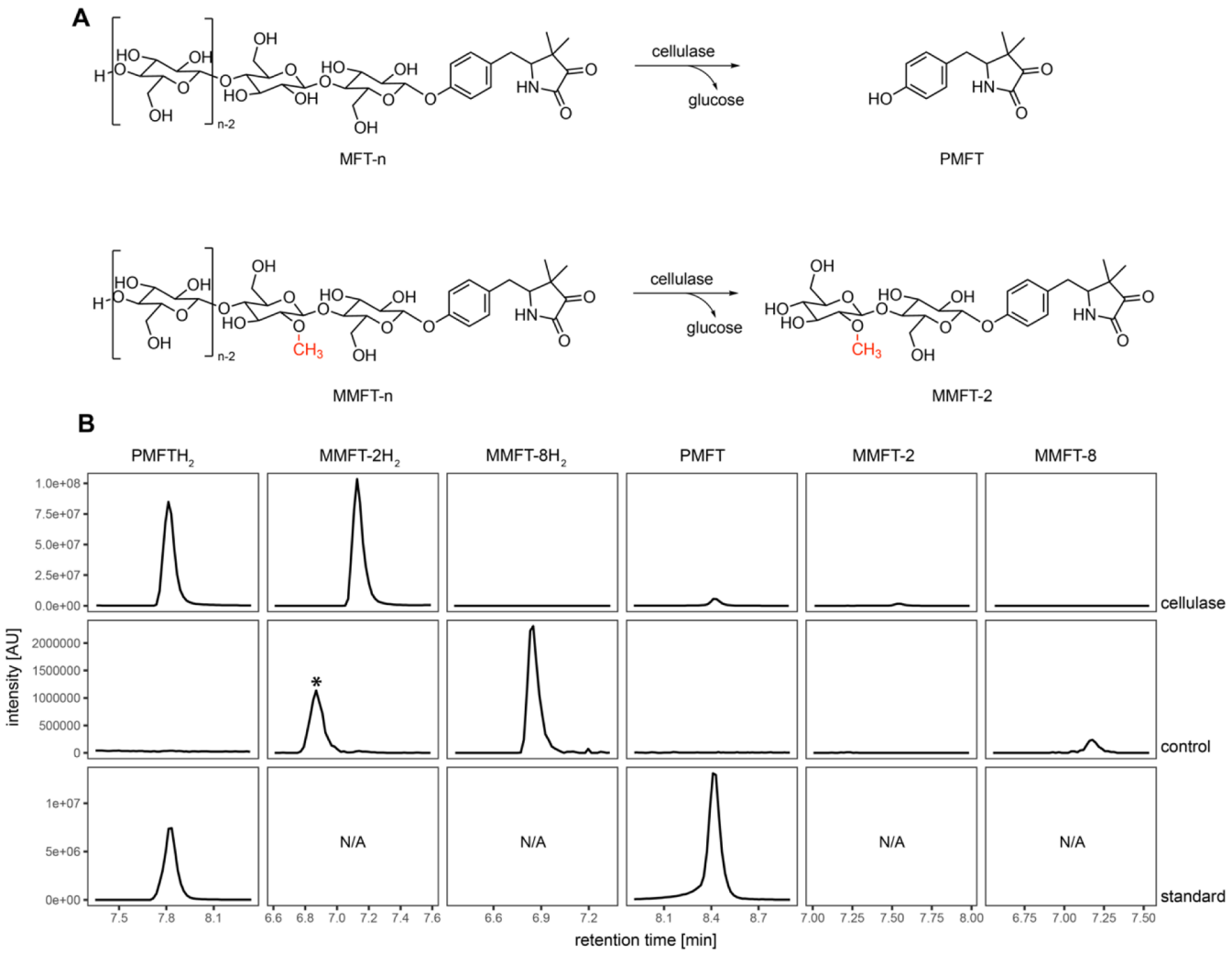

Figure 6. Methylation of MFT protects the cofactor from cellulases in vitro. (A) Scheme showing the degradation of the β-1,4-glucan chain of mycofactocins by cellulases. While non-methylated mycofactocins are degraded to aglycone, methylmycofactocins are protected at the site of methylation. (B) Stacked EICs of representative mycofactocin congeners in *M. smegmatis* metabolome extracts before and after treatment with a cellulase mixture. The increase in the intensity of the aglycone originates from degraded mycofactocinols, while the increase in methylmycofactocinol-2 originates from methylmycofactocinol-*n* (with $n > 2$). Asterisk: secondary peaks not aligning with the expected retention co-elute with higher glycosylated mycofactocin congeners and therefore can be explained as in-source fragmentation products of the latter. EIC data (5 ppm window): premycofactocinol ($C_{13}H_{17}NO_3$, RT: 7.84 min, *m/z* 236.1281 $[M + H]^+$), methylmycofactocinone-2 ($C_{26}H_{37}NO_{13}$, RT: 7.47 min, *m/z* 572.2338 $[M + H]^+$), methylmycofactocinone-8 ($C_{62}H_{97}NO_{43}$, RT: 7.18 min, *m/z* 1544.5507 $[M + H]^+$), premycofactocinone ($C_{13}H_{15}NO_3$, RT: 8.40 min, *m/z* 234.1125 $[M + H]^+$), methylmycofactocinol-2 ($C_{26}H_{39}NO_{13}$, RT: 7.10 min, *m/z*: 574.2494 $[M + H]^+$), and methylmycofactocinol-8 ($C_{62}H_{99}NO_{43}$, RT: 6.81 min, *m/z* 1546.5664 $[M + H]^+$).

stops right at the 2-*O*-methylated glucose moiety, indicating that methylmycofactocins (MMFT-2 and MMFT-2H_2) exert stability against the action of cellulases, while non-methylated counterparts are easily digested (Figure 6A). The cellulase treatments also indicate that the β-1,4-linkage of the glycosylation as well as the position of the methyl group are conserved in all methylmycofactocin producers investigated in this study.

The question of whether this protective effect plays a role in vivo in some organisms will be further investigated in future studies. Notably, we did not observe any accumulation of the cellulase degradation product methylmycofactocin-2 or any aglycones during the growth experiments conducted with *M. smegmatis* (Figures S17 and S18). Therefore, we do not expect the protective effect to play a major role in this context. It might, however, become relevant under certain environmental conditions. It should be mentioned that mycobacteria possess a widespread gene encoding a (secreted) cellulase, including the experimentally characterized representatives of *M. smegmatis* (MSMEG_6752)[18] and *M. tuberculosis* (Rv0062).[19] However, the occurrence of this cellulase gene in an organism was not correlated with MFT methylation. It is, however, tempting to speculate that the co-expression of genes encoding glycoside hydrolases targeting β-1,4-glucans together with MFT genes could lead to an undesired degradation of the cofactor. This might have been a driving force for the evolution of MFT methylation as a protection mechanism as well as its conservation in certain bacterial species. Later in evolution, other enzymes or regulators might have adapted to the modification.

Notably, other cofactors have undergone modifications in their "tail-moieties" during evolution. An extreme example is the phosphorylation of NAD to NADP by NAD kinase.[20] Here, the phosphorylation enables specific and mutually

https://doi.org/10.1021/acschembio.2c00659
ACS Chem. Biol. 2022, 17, 3207−3217

exclusive interactions of enzymes with one of the two cofactors so that two distinct redox pools with different reduced/oxidized ratios can be formed in the same cell. We could not observe any obvious split of the redox pool between MFTs and MMFTs in our datasets; that is, the ratio of reduced to oxidized non-methylated mycofactocins ($MFTH_2$/MFT) was comparable to the ratio of their corresponding methylated forms ($MMFTH_2$/MMFT) (Figure S19). While NAD and NADP are seen as distinct cofactors, there are other less prominent diversifications of tail moieties, for instance, folate and co-enzyme F_{420}, which are typically decorated with γ-linked glutamate residues but are capped with α-linked glutamate in some species.[21,22] The archaeal cofactor methanofuran has only γ-linked glutamates, but the chain can be interrupted by an unusual building block in certain methanococcales.[23] Furthermore, methylofuran, a cofactor involved in methylotrophy, was shown to contain a mixture of γ-linked and α-linked glutamate residues.[24] While the protection against peptidase activities might play a role in these examples, the physiological function of these modifications, however, remains elusive.

■ CONCLUSIONS

We discovered the gene encoding the SAM-dependent methyltransferase MftM is responsible for methylation of the glycoside moiety of mycofactocin in *M. smegmatis*. Based on metabolic profiling and bioinformatics, we provide further evidence that homologous genes/enzymes present in other MFT producers fulfill the same biochemical function and typically co-occur, not only with MFT biosynthesis but also with the MFT-associated alcohol dehydrogenase Mdo. Furthermore, we revealed an extended lag phase combined with delayed MFT biosynthesis in methyltransferase deficient mutants of *M. smegmatis* when grown on ethanol. We also demonstrate that the methylation of MFT confers resistance against digestion by cellulases in vitro. It remains unclear if or to what extent the enhanced stability alone can account for the altered growth phenotype. However, this work provides a stable foundation for future studies into the potentially diverse functions of MFT methylation in vivo.

■ METHODS

Bacterial Strains and Cultivation Methods. The following strains were obtained from the Jena Microbial Resource Collection (JMRC): *A. methanolica* 239 (DSM 44096), *Mycolicibacterium smegmatis* mc^2 155, *S. erythraea* NRRL 2338, and *R. erythropolis* DSM 43060. *Escherichia coli* TOP10 was purchased from Invitrogen (Thermo Fisher Scientific). *E. coli* strains and *M. smegmatis* were cultivated at 37 °C, while all of the other strains were cultivated at 30 °C. *M. smegmatis* strains were cultivated on lysogeny broth (LB; tryptone 10 g L^{-1}, sodium chloride 8 g L^{-1}, and yeast extract 5 g L^{-1}) supplemented with 0.05% (w/v) Tween 80 (LB-Tween) for liquid cultures. For the cultivation of mutants, media were supplemented with hygromycin B (50 μg mL^{-1}); for the complementary mutant, kanamycin was added (50 μg mL^{-1}). *E. coli* TOP10 (+ plasmids) was cultivated on LB supplemented with either hygromycin B (100 μg mL^{-1}) or kanamycin (50 μg mL^{-1}). All other strains were cultivated on glucose-yeast-malt *Streptomyces* medium (GYM; glucose 4 g L^{-1}, yeast extract 4 g L^{-1}, malt extract 10 g L^{-1}, and $CaCO_3$ 2 g L^{-1}). Liquid cultures were incubated under agitation at 210 rpm (25 mm throw), and solid media contained 1.5% (w/v) agar−agar. The experiments with the *M. bovis* BCG strain DSM 43990 and the *M. tuberculosis* strain H37Rv were conducted in BSL2 and BSL3 facilities, respectively, at Friedrich-Loeffler-Institut, Jena.

Genetic Manipulation of *M. smegmatis*. The gene deletion mutants Δ*MSMEG_1650*::Hyg^r (Δ*MSMEG_1650*), Δ*MSMEG_1771*::Hyg^r (Δ*MSMEG_1771*), Δ*MSMEG_5176*::Hyg^r (Δ*MSMEG_5176*), Δ*MSMEG_6235*::Hyg^r (Δ*MSMEG_5354*), Δ*MSMEG_6237*, and Δ*MSMEG_6663*::Hyg^r (Δ*MSMEG_6663*) were obtained using the pML2424 system.[25] The plasmid vectors for gene deletion were generated by amplifying ca. 1500 bp in each of the up- and down-stream regions of the target gene from *M. smegmatis* genomic DNA using oligonucleotides described in Table S2. The Q5 High-Fidelity DNA polymerase with Q5 High GC Enhancer was used according to the manufacturer's instructions (New England Biolabs). The amplicons were inserted before and after the GFP-hygromycin resistance cassette of pML2424, respectively, using *E. coli* TOP10 as a cloning strain. To obtain a markerless gene deletion mutant for *MSMEG_6237*, the hygromycin cassette flanked by *LoxP* sites was removed from the genome of the temporary strain Δ*MSMEG_6237*::Hyg^r via recombination by Cre recombinase (encoded on pML2714), yielding Δ*MSMEG_6237* (Δ*mftM*) as described before.[25] The complementation strain Δ*mftM attB*::pME31 (Δ*mftM*-comp) was obtained using plasmids derived from the integrative pMCpAINT vector.[26] The complementation plasmid (pME31) was obtained by cloning *mftM* with its 100 bp upstream (putative) promotor region amplified from *M. smegmatis* genomic DNA using oligonucleotides described in Table S2. Cells were prepared for electroporation using a modified protocol by Cirillo et al.[27] LB-Tween was used as a medium, and if required, it was supplemented with hygromycin B; the cultures were prepared for competence with an optical density at 600 nm (OD_{600}) of 1.8, and aliquots of 200 μL were used for transformation. Electrocompetent cells were transformed with 500 ng of plasmid through electroporation using cuvettes with a 2 mm gap and an exponentially decaying pulse of 2.5 kV, 25 μF, and 1 kΩ. Immediately after pulse application, 800 μL of LB-Tween was added, and the cells were transferred to a 50 mL conical centrifuge tube. The cells were recovered for 2 h at 37 °C and 210 rpm and plated on solid LB medium supplemented with antibiotics as described above.

Cultivation of Non-pathogenic Bacteria for Metabolomics and Growth Experiments. Strains were first grown in liquid preculture as described for maintenance cultivation, followed by a second preculture in adapted Hartmans de Bont medium (HdB; $(NH_4)_2SO_4$ 2 g L^{-1}, $MgCl_2{\cdot}6H_2O$ 0.1 g L^{-1}, Na_2HPO_4 anhydrous 3 g L^{-1}, and KH_2PO_4 anhydrous 1.07 g L^{-1}) supplemented with 1% (w/v) glucose, 0.2% (v/v) 500 × trace element solution (ethylenediaminetetraacetic acid 5 g L^{-1}, $CaCl_2{\cdot}2H_2O$ 0.5 g L^{-1}, $Na_2MoO_4{\cdot}2H_2O$ 0.1 g L^{-1}, $CoCl_2{\cdot}6H_2O$ 0.2 g L^{-1}, $MnCl_2{\cdot}2H_2O$ 0.5 g L^{-1}, $ZnSO_4{\cdot}7H_2O$ 1 g L^{-1}, $FeSO_4{\cdot}7H_2O$ 2.5 g L^{-1}, and $CuSO_4{\cdot}5H_2O$ 0.1 g L^{-1}),[28] and—if suitable—including antibiotics as described above. Cells of the second preculture were washed once with plain HdB medium (no antibiotics or carbon sources) before inoculation of the main culture. This preculture was used to inoculate 50 mL of main HdB cultures containing 2% ethanol (v/v) in 250 mL shake flasks closed with breathable rayon membranes (VWR) at an initial OD_{600} of 0.1. For the cultivation of *M. smegmatis*, the HdB medium was supplemented with 0.05% (w/v) of tyloxapol (Sigma-Aldrich). *M. smegmatis* and *R. erythropolis* were incubated by shaking at 210 rpm, while *A. methanolica* and *S. erythraea* were incubated as stationary liquid cultures. Stable isotope labeling was performed using *M. smegmatis* with 1 mM L-tyrosine-$^{13}C_9$ (99% atom purity, Cortecnet), 1 mM L-methionine-(methyl-^{13}C) (99% atom purity, Sigma-Aldrich), and 1 mM L-valine-$^{13}C_5$ (99% atom purity, Merck) as described.[15]

The growth of bacteria was monitored using the backscattered light method of the cell growth quantifier device (Aquila Biolabs). Data from the quadruplicates were merged using the CG Quant software to obtain the mean and standard deviation of the cultures, and growth curves were plotted using R.

Extraction of Intracellular Metabolites from Non-pathogenic Bacteria and *M. smegmatis*. Bacteria were cultivated as described above, if not indicated otherwise, until the beginning of the stationary growth phase as described with modifications.[15] Briefly, a

https://doi.org/10.1021/acschembio.2c00659
ACS Chem. Biol. 2022, 17, 3207−3217

0.22 μM cellulose-acetate membrane filter (Ø 47 mm, Sartorius) was washed three times with 10 mL of ultrapure water, each using a vacuum filtration unit (Sartorius), followed by the addition of 10 mL of cell culture per OD_{600} unit and washing of the cells three times with 10 mL of ultrapure water. The filter with cells was transferred immediately to a bottle containing 20 mL of extraction mixture chilled to −20 °C consisting of acetonitrile, methanol, water, and formic acid (60:20:19.9:0.1 (v/v), LC−MS grade, VWR). Cells were disrupted by three freeze−thaw cycles, that is, for 1 h at −70 °C, followed by 5 min of sonication in an ultrasonic bath (Bandelin). The extracts were transferred to glass flasks and lyophilized at 1 mbar and −90 °C, followed by reconstitution in a total of 1 mL of water (LC−MS grade, VWR). The extracts were prepared for LC−MS measurement by centrifugation for 20 min at 17,000*g* and room temperature to remove cell debris, followed by transfer of the supernatant to a fresh tube and centrifugation for 20 min at 17,000*g* and room temperature. Extracts were stored at −20 °C until measurement.

Extraction of Extracellular Metabolites from *M. smegmatis*. Bacteria were cultivated as described above. 2 ml of culture was centrifuged for 3 min at 6500*g* and room temperature. The supernatant was processed using a 1 mL/100 mg C18 solid-phase extraction column (Macherey-Nagel, CHROMABOND). Bound analytes were eluted with 500 μL of water/methanol 50:50 (v/v), followed by elution with 500 μL of methanol. The fractions were combined and dried under reduced pressure at 60 °C. The dried extract was reconstituted in 200 μL water and subjected to LC−MS/MS analysis as described below. All solvents used were LC−MS grade (VWR). Data were normalized to the cell density using the OD_{600} of the cultures.

Cultivation and Extraction of *M. tuberculosis* and *M. bovis* for Metabolomics Studies. Pure colonies of each strain were used to inoculate 3 mL of Middlebrook broth (7H9 [Difco] supplemented with 1% (w/v) cholesterol dissolved in either 1% (v/v) ethanol or 0.1% (v/v) DMSO and OADC [oleic acid albumin dextrose complex, Becton Dickinson], in house preparation) and incubated (static conditions, 37 °C, 2−4 weeks). Solubilization of cultures and disruption of clumps were carried out by passaging the culture at least three times through a sterile needle. Six individual 15 mL conical tubes with 10 mL of Middlebrook broth each were inoculated with 500 μL of culture and incubated (static conditions, 37 °C, closed cap). Weekly, 100 μL of absolute ethanol was added to three of the six cultures of each strain, while three cultures remained as controls without ethanol supplementation. In the fifth week, the cultures were centrifuged (4100*g*, 20 min, 20 °C), the supernatant was discarded, and the pellet was resuspended in 2 mL of water (LC−MS grade, VWR). The suspension was autoclaved at 121 °C for 20 min and stored at −70 °C until further processing. Before and after sterilization, samples of the suspension were taken and incubated on Löwenstein-Jensen agar slants with glycerol (Artelt-Enclit) at 37 °C at least 4 weeks for confirmation of bacterial inactivation. Inactivated cell extracts were centrifuged (17,000*g*, 20 min, room temperature). The supernatant was transferred to a new tube and centrifuged again. The extract was stored in a glass vial at −20 °C until LC−MS measurements.

LC−MS/MS Measurements. LC−MS measurements were performed on a Dionex UltiMate 3000 UHPLC connected to a Q Exactive Plus mass spectrometer (Thermo Fisher Scientific) as described[15] using a mobile phase consisting of A—water + 0.1% (v/v) formic acid—and B—acetonitrile + 0.1% (v/v) formic acid—and the following gradient at 300 μL min^{-1}: 0−2 min 2% B, 2−10 min 2−62.5% B, 10−10.5 min 62.5−99% B, 10.5−13.5 min 99% B, 13.5−18.5 min 99−2% B, and 18.5−22 min 2% B. High-resolution mass spectra were acquired in a positive ionization mode in a scan range of m/z 200−2000 as MS^1 data with highe- energy C-trap dissociation fragmentation of the 10 most abundant ions per MS^1 scan (MS^1-$ddMS^2$ TOP10) using a normalized collision energy of 40 arbitrary units. Data analysis was performed with Mzmine 2 (version 2.53)[29] at an m/z tolerance of ≤5 parts per million (ppm) for MS^1 data and ≤10 ppm for MS^2 data. Statistical analysis and plotting were achieved using R (version 4.2.0) in combination with the tidyverse package.[30]

Cellulase Treatment of Metabolite Extracts. Metabolite extracts were prepared as described above and incubated for 2 h at 37 °C with cellulase (20 μg mL^{-1}) from *Trichoderma reesei* ATCC 26921 containing β-glucosidase, cellobiosidase I and II, and *endo*-β-1,4-glucanase (Sigma-Aldrich) diluted from a 200 μg mL^{-1} stock solution in ultrapure water. The reaction was quenched at 95 °C for 10 min. As a control, the cellulase was replaced with the same volume of ultrapure water. LC−MS measurements of reaction products were performed as described above. Aglycones were confirmed by comparison to synthetic standards (see below).

Gene Similarity Searches and Co-Occurrence Analysis. See Supporting Information—additional experimental procedures.

Chemical Synthesis of PMFT and $PMFTH_2$ Standards. See Supporting Information—additional experimental procedures.

■ ASSOCIATED CONTENT

Supporting Information

The Supporting Information is available free of charge at https://pubs.acs.org/doi/10.1021/acschembio.2c00659.

Co-occurrence of genes encoding MftC, MftM, and Mdo homologues in microbial genomes; organism names and accession numbers of MftC, MftM, and Mdo homologues found in these organisms; use of table to construct the Venn diagram shown in Figure 4; and occurrence per genus of MftM and Mdo in genomes of MFT producers in percent (XLSX)

Additional LC−MS data of bacterial samples and the description of bioinformatics procedures as well as chemical synthesis of PMFT and $PMFTH_2$ standards along with spectral data of synthetic material (additional experimental procedures) (PDF)

■ AUTHOR INFORMATION

Corresponding Author

Gerald Lackner − *Junior Research Group Synthetic Microbiology, Leibniz Institute for Natural Product Research and Infection Biology—Hans Knöll Institute, 07745 Jena, Germany*; orcid.org/0000-0002-0307-8319; Email: gerald.lackner@leibniz-hki.de

Authors

Mark Ellerhorst − *Junior Research Group Synthetic Microbiology, Leibniz Institute for Natural Product Research and Infection Biology—Hans Knöll Institute, 07745 Jena, Germany*; orcid.org/0000-0001-6058-2522

Stefanie A. Barth − *Friedrich-Loeffler-Institut—Federal Research Institute for Animal Health (FLI), Institute of Molecular Pathogenesis, 07743 Jena, Germany*

Ana Patrícia Graça − *Junior Research Group Synthetic Microbiology, Leibniz Institute for Natural Product Research and Infection Biology—Hans Knöll Institute, 07745 Jena, Germany*

Walid K. Al-Jammal − *Institute of Organic Chemistry and Macromolecular Chemistry, Friedrich Schiller University Jena, 07743 Jena, Germany*

Luis Peña-Ortiz − *Junior Research Group Synthetic Microbiology, Leibniz Institute for Natural Product Research and Infection Biology—Hans Knöll Institute, 07745 Jena, Germany*; orcid.org/0000-0002-0867-9471

Ivan Vilotijevic − *Institute of Organic Chemistry and Macromolecular Chemistry, Friedrich Schiller University Jena, 07743 Jena, Germany*; orcid.org/0000-0001-6199-0632

Complete contact information is available at:
https://pubs.acs.org/10.1021/acschembio.2c00659

Funding
We thank the Carl Zeiss Foundation for funding (GL and PG). Financial support from Friedrich Schiller University Jena and DAAD (graduate fellowship to W.K.A.J.) is gratefully acknowledged.

Notes
The authors declare no competing financial interest.
ME performed research (genetics, metabolomics, and bioinformatics), analyzed data, and drafted the manuscript. PG designed and conducted research (genetics, Mtb experiments). SAB conducted research (Mtb experiments). WKA designed and conducted research (synthesis) and analyzed data. LP performed research (^{13}C-labeling). IV designed research, analyzed data, and wrote parts of the manuscript (chemical synthesis). GL designed research, analyzed data, and edited the manuscript.

■ ACKNOWLEDGMENTS
Plasmids pML2424 and pML2714 were kindly provided by M. Niederweis (University of Alabama at Birmingham). We thank P. Bellstedt and N. Ueberschaar for their support with NMR and MS analysis.

■ REFERENCES
(1) Krishnamoorthy, G.; Kaiser, P.; Lozza, L.; Hahnke, K.; Mollenkopf, H. J.; Kaufmann, S. H. E. Mycofactocin is associated with ethanol metabolism in mycobacteria. *mBio* **2019**, *10*, No. e00190.
(2) Dubey, A. A.; Jain, V. Mycofactocin is essential for the establishment of methylotrophy in *Mycobacterium smegmatis*. *Biochem. Biophys. Res. Commun.* **2019**, *516*, 1073−1077.
(3) Ostrovsky, M. Endogenous ethanol-Its metabolic, behavioral and biomedical significance. *Alcohol* **1986**, *3*, 239−247.
(4) Mehta, A. J.; Guidot, D. M. Alcohol and the Lung. *Alcohol. Res.* **2017**, *38*, 243−254.
(5) Krishnamoorthy, G.; Kaiser, P.; Constant, P.; Abu Abed, U.; Schmid, M.; Frese, C. K.; Brinkmann, V.; Daffé, M.; Kaufmann, S. H. E. Role of premycofactocin synthase in growth, microaerophilic adaptation, and metabolism of Mycobacterium tuberculosis. *mBio* **2021**, *12*, No. e0166521.
(6) Mendauletova, A.; Latham, J. A. Biosynthesis of the redox cofactor mycofactocin is controlled by the transcriptional regulator MftR and induced by long-chain acyl-CoA species. *J. Biol. Chem.* **2022**, *298*, 101474.
(7) Ayikpoe, R.; Govindarajan, V.; Latham, J. A. Occurrence, function, and biosynthesis of mycofactocin. *Appl. Microbiol. Biotechnol.* **2019**, *103*, 2903−2912.
(8) Haft, D. H. Bioinformatic evidence for a widely distributed, ribosomally produced electron carrier precursor, its maturation proteins, and its nicotinoprotein redox partners. *BMC Genomics* **2011**, *12*, 21.
(9) Khaliullin, B.; Aggarwal, P.; Bubas, M.; Eaton, G. R.; Eaton, S. S.; Latham, J. A. Mycofactocin biosynthesis: modification of the peptide MftA by the radical S-adenosylmethionine protein MftC. *FEBS Lett.* **2016**, *590*, 2538−2548.
(10) Bruender, N. A.; Bandarian, V. The radical S-adenosyl-L-methionine enzyme MftC catalyzes an oxidative decarboxylation of the C-terminus of the MftA peptide. *Biochemistry* **2016**, *55*, 2813−2816.
(11) Khaliullin, B.; Ayikpoe, R.; Tuttle, M.; Latham, J. A. Mechanistic elucidation of the mycofactocin-biosynthetic radical S-adenosylmethionine protein, MftC. *J. Biol. Chem.* **2017**, *292*, 13022−13033.
(12) Bruender, N. A.; Bandarian, V. The creatininase homolog MftE from *Mycobacterium smegmatis* catalyzes a peptide cleavage reaction in the biosynthesis of a novel ribosomally synthesized post-translationally modified peptide (RiPP). *J. Biol. Chem.* **2017**, *292*, 4371−4381.
(13) Ayikpoe, R.; Salazar, J.; Majestic, B.; Latham, J. A. Mycofactocin Biosynthesis Proceeds through 3-Amino-5-[(p-hydroxyphenyl)methyl]-4,4-dimethyl-2-pyrrolidinone (AHDP); Direct Observation of MftE Specificity toward MftA*. *Biochemistry* **2018**, *57*, 5379−5383.
(14) Ayikpoe, R. S.; Latham, J. A. MftD Catalyzes the Formation of a Biologically Active Redox Center in the Biosynthesis of the Ribosomally Synthesized and Post-translationally Modified Redox Co-factor Mycofactocin. *J. Am. Chem. Soc.* **2019**, *141*, 13582−13591.
(15) Peña-Ortiz, L.; Graça, A. P.; Guo, H. J.; Braga, D.; Köllner, T. G.; Regestein, L.; Beemelmanns, C.; Lackner, G. Structure elucidation of the redox co-factor mycofactocin reveals oligo-glycosylation by MftF. *Chem. Sci.* **2020**, *11*, 5182−5190.
(16) Ripoll-Rozada, J.; Costa, M.; Manso, J. A.; Maranha, A.; Miranda, V.; Sequeira, A.; Ventura, M. R.; Macedo-Ribeiro, S.; Pereira, P. J. B.; Empadinhas, N. Biosynthesis of mycobacterial methylmannose polysaccharides requires a unique 1- O -methyltransferase specific for 3- O -methylated mannosides. *Proc. Natl. Acad. Sci. U. S. A.* **2019**, *116*, 835−844.
(17) Singh, S.; McCoy, J. G.; Zhang, C.; Bingman, C. A.; Phillips, G. N., Jr.; Thorson, J. S. Structure and Mechanism of the Rebeccamycin Sugar 4′-O-Methyltransferase RebM. *J. Biol. Chem.* **2008**, *283*, 22628−22636.
(18) Van Wyk, N.; Navarro, D.; Blaise, M.; Berrin, J. G.; Henrissat, B.; Drancourt, M.; Kremer, L. Characterization of a mycobacterial cellulase and its impact on biofilm- and drug-induced cellulose production. *Glycobiology* **2017**, *27*, 392−399.
(19) Varrot, A.; Leydier, S.; Pell, G.; Macdonald, J. M.; Stick, R. V.; Henrissat, B.; Gilbert, H. J.; Davies, G. J. *Mycobacterium tuberculosis* strains possess functional cellulases. *J. Biol. Chem.* **2005**, *280*, 20181−20184.
(20) Agledal, L.; Niere, M.; Ziegler, M. The phosphate makes a difference: cellular functions of NADP. *Redox Rep.* **2010**, *15*, 2−10.
(21) Graupner, M.; White, R. H. Methanococcus jannaschii Coenzyme F 420 Analogs Contain a Terminal α-Linked Glutamate. *J. Bacteriol.* **2003**, *185*, 4662−4665.
(22) Ferone, R.; Hanlon, M. H.; Singer, S. C.; Hunt, D. F. alpha-Carboxyl-linked glutamates in the folylpolyglutamates of *Escherichia coli*. *J. Biol. Chem.* **1986**, *261*, 16356−16362.
(23) Allen, K. D.; White, R. H. Identification of structurally diverse methanofuran co-enzymes in methanococcales that are both *N*-formylated and *N*-acetylated. *Biochemistry* **2014**, *53*, 6199−6210.
(24) Hemmann, J. L.; Saurel, O.; Ochsner, A. M.; Stodden, B. K.; Kiefer, P.; Milon, A.; Vorholt, J. A. The One-carbon Carrier Methylofuran from Methylobacterium extorquens AM1 Contains a Large Number of α- and γ-Linked Glutamic Acid Residues. *J. Biol. Chem.* **2016**, *291*, 9042−9051.
(25) Ofer, N.; Wishkautzan, M.; Meijler, M.; Wang, Y.; Speer, A.; Niederweis, M.; Gur, E. Ectoine biosynthesis in *Mycobacterium smegmatis*. *Appl. Environ. Microbiol.* **2012**, *78*, 7483−7486.
(26) Warner, D. F.; Ndwandwe, D. E.; Abrahams, G. L.; Kana, B. D.; Machowski, E. E.; Venclovas, C.; Mizrahi, V. Essential roles for imuA′- and imuB -encoded accessory factors in DnaE2-dependent mutagenesis in Mycobacterium tuberculosis. *Proc Natl Acad Sci U S A* **2010**, *107*, 13093−13098.
(27) Cirillo, J. D.; Weisbrod, T. R.; Jacobs, W. R., Jr. Efficient electrotransformation of *Mycobacterium smegmatis*. *Bio-Rad US/EG Bull* **1993**, *1360*, 1−4.
(28) Berney, M.; Weimar, M. R.; Heikal, A.; Cook, G. M. Regulation of proline metabolism in mycobacteria and its role in carbon metabolism under hypoxia. *Mol. Microbiol.* **2012**, *84*, 664−681.
(29) Pluskal, T.; Castillo, S.; Villar-Briones, A.; Orešič, M. MZmine 2: modular framework for processing, visualizing, and analyzing mass spectrometry-based molecular profile data. *BMC Bioinformatics* **2010**, *11*, 395.

(30) Wickham, H.; Averick, M.; Bryan, J.; Chang, W.; McGowan, L.; François, J.; Grolemund, G.; Hayes, A.; Henry, L.; Hester, J.; Kuhn, M.; Pedersen, T. L.; Miller, E.; Bache, S. M.; Müller, K.; Ooms, J.; Robinson, D.; Seidel, D. P.; Spinu, V.; Takahashi, K.; Vaughan, D.; Wilke, C.; Woo, K.; Yutani, H. Welcome to the Tidyverse. *J. Open Source Softw.* **2019**, *4*, 1686.

https://doi.org/10.1021/acschembio.2c00659
ACS Chem. Biol. 2022, 17, 3207−3217